American Mineralogist, Volume 62, pages 634–645, 1977

Zoned titanian augite in alkali olivine basalt from Tahiti and the nature of titanium substitutions in augite

ROBERT J. TRACY[1] AND PETER ROBINSON

Department of Geology, University of Massachusetts,
Amherst, Massachusetts 01002

Abstract

Alkali olivine basalt from Tahiti contains zoned titanaugite microphenocrysts, phenocrysts, and overgrowths on lherzolite xenoliths, plus olivine (Fo_{88-49}), plagioclase (An_{61-27}), alkali feldspar (Or_{72}), leucite, titanomagnetite ($Mag_{30}\ Usp_{70}$), and ilmenite ($Ilm_{94}\ Hem_6$). Augite rims contain up to 8.8 weight percent TiO_2, the most Ti-rich yet documented from earth, accompanied by very low SiO_2 (37.3 wt%) and high Al_2O_3 (13.6 wt%). Pyroxene stoichiometry suggests a modest amount of Fe is Fe^{3+}, and leads to the following formulas for low- and high-Ti augites respectively:

$$(Na_{0.04}Ca_{0.84}Mn_{0.01}Fe^{2+}_{0.11})(Fe^{2+}_{0.05}Mg_{0.83}Fe^{3+}_{0.04}Cr_{0.03}Ti^{4+}_{0.03}Al_{0.03})(Al_{0.10}Si_{1.90})O_6$$
$$(Na_{0.07}Ca_{0.89}Mn_{0.01}Fe^{2+}_{0.03})(Fe^{2+}_{0.17}Mg_{0.43}Fe^{3+}_{0.10}Cr_{0.00}Ti^{4+}_{0.25}Al_{0.05})(Al_{0.57}Si_{1.43})O_6$$

The Tahiti composition trend suggests substitution of $Fe^{2+}+Ti^{4+}+2Al$ for $2Mg+2Si$, leading to the idealized end-member $CaFe_{0.5}Ti^{4+}_{0.5}AlSiO_6$. By contrast, stoichiometry and spectral data of high-Ti augites from the Moon (up to 9.3 wt% TiO_2) and Allende meteorite (up to 17.7 wt% TiO_2) indicate that half or more of the Ti is Ti^{3+}. Thus, although the Allende augites are much richer in Ti (with much as $CaTi^{3+}AlSiO_6$), the Tahiti specimens are the most *titanian* yet reported. Magmatic conditions at Tahiti which favored crystallization of titanian augite included low P, high TiO_2, low SiO_2, high Ca/Al and Mg/Fe ratios, and low fO_2. Coexisting magnetite–ilmenite indicate $\log fO_2 = -11$ atm at 1020°C, slightly more reducing than FMQ buffer, but much more oxidizing than lunar and Allende meteorite conditions.

Introduction

Recently Mason (1974) reported on aluminum- and titanium-rich pyroxenes, with special reference to the Allende meteorite, and noted the most Ti-rich pyroxenes reported from Earth. In this paper, we present analyses of zoned titanaugites in alkali basalt from Papeete, Tahiti, which exceed previously reported terrestrial augites in Ti content. The most Ti-rich augites from Tahiti are as titaniferous as those reported from lunar basalts. The strikingly large titanium content of the Tahitian augites led us to examine chemical trends in Ti-rich augites, and to review the nature of titanium substitutions in augite.

The most Ti-rich terrestrial augite previously reported (Dixon and Kennedy, 1933) contains 5.7 weight percent TiO_2 and occurs in a calc-silicate hornfels in Scotland. Titanaugites in mafic and alkalic igneous rocks have TiO_2 contents approaching this value (Deer *et al.*, 1963).[2] Approximate limits for observed Ti content of lunar augites appear to be 9.3 weight percent TiO_2 for Apollo 11 (Bunch *et al.*, 1970) and 8.5 weight percent for Apollo 17 (Brown *et al.*, 1975). The most Ti-rich pyroxenes yet reported are from the Allende meteorite and contain up to 22 weight percent TiO_2 (Fuchs, 1971; Mason, 1974; S. E. Haggerty, personal communication, 1976).

Location and petrography

The island of Tahiti lies west of the East Pacific Rise, near 17°S latitude and 149°W longitude. It is part of the Society Islands volcanic chain and was

---

[1] Present address: Department of Geological Sciences, Harvard University, Cambridge, Massachusetts 02138.

[2] Lebedev and Lebedev (1934) report 8.97 weight percent TiO_2 in titanaugite from an ilmenite pyroxenite ore body, but the low SiO_2, CaO, and MgO, and high FeO which they report suggest that their pyroxene separate was contaminated with ilmenite.

volcanically active during much of the later part of the Cenozoic, according to Dymond (1975), who reports K–Ar ages of about 0.6 to 1.0 m.y. for a number of the alkaline lavas. The geology of Tahiti, described by Williams (1933) and McBirney and Aoki (1968), consists of a plutonic core surrounded by a deeply dissected volcanic shield of dominantly alkali-rich, undersaturated lavas. The plutonic core apparently represents very late magmas which intruded the central volcanic vents and crystallized as much as 2 or 3 km below the volcano summit (McBirney and Aoki, 1968).

The samples of this study were collected by Robinson in 1968 from boulders in the bed of Faataua River in Papeete. The rock is hypabyssal or extrusive ankaramite. Dunite and spinel lherzolite nodules occur in the samples and are described elsewhere (Tracy and Robinson, 1975; in preparation). Major phases in the ankaramite include olivine, titanaugite, and plagioclase, with subordinate amounts of titanomagnetite, ilmenite, apatite, K–feldspar, leucite and glass. Compositions of phases determined by microprobe are summarized in Table 1. An electron-probe analysis of a fused sample of this basalt, a bulk chemical analysis of a typical Tahiti ankaramite (McBirney and Aoki, 1968), and a probe analysis of interstitial devitrified glass (probable late liquid) are also given. The compositions of coexisting titanomagnetite and ilmenite phenocrysts (Table 1), recalculated according to the method of Buddington and Lindsley (1964), yield an estimate of equilibration temperature of 1020°C and an fO_2 of 10^{-11} atomspheres (Buddington and Lindsley, 1964, Fig. 5), indicating equilibration conditions slightly more reducing than the quartz–fayalite–magnetite buffer.

Titanaugite occurs in two principal modes—as phenocrysts (Fig. 1a) and as overgrowths on spinel lherzolite xenoliths (Fig. 1b). These overgrowths occur only where pyroxene rather than olivine forms the periphery of the xenolith, apparently because of favorable nucleation sites provided by the pyroxene lattice. The overgrowths show strong outward zoning from colorless low-Ti augite through deep brownish-purple titanaugite with up to 7 weight percent TiO_2. Dominantly euhedral titanaugite phenocrysts range from about 5 to 500 microns in size, and display both concentric zoning and, much less commonly, sector-zoning. The scarcity of chemically or optically distinct sector-zoning is surprising, in view of its common occurrence in Ti-rich augites (Strong, 1969; Hollister and Gancarz, 1971). Where sector-zoning is observed, the darker purple, more Ti-rich composition is confined to the prism sector (100), as has been noted for other occurrences (Hollister and Gancarz, 1971). Titanaugites richest in titanium seem to occur adjacent to areas of fine-grained groundmass which

Table 1. Compositions of phases in Tahitian alkali olivine basalt and basalt bulk chemistry

Mineral	Composition[1]		Bulk Composition		
Olivine	Fo_{88} - Fo_{49}	SiO_2	43.26[2]	41.8[3]	53.4[4]
		TiO_2	3.40	2.7	1.1
Plagioclase	$An_{61}Ab_{36}Or_3$ - $An_{27}Ab_{64}Or_9$	Al_2O_3	9.69	9.9	22.2
		Cr_2O_3	na	0.1	0
Titanomagnetite	$(Fe^{2+}_{.80}\ Mg_{.17}\ Mn_{.03})(Fe^{2+}_{.67}\ Fe^{3+}_{.46}\ Ti^{4+}_{.70}\ Al_{.16}\ Cr_{.01})O_4$	FeO	12.26	12.0	4.1
		MnO	0.16	0.2	0.1
Ilmenite	$Ilm_{94}Hem_6$ (MgO ≅ 2 wt.%)	MgO	12.64	18.9	1.6
		CaO	12.10	10.4	0.8
K-feldspar	$An_2Ab_{26}Or_{72}$	Na_2O	1.59	2.3	8.8
		K_2O	1.18	1.1	7.9
Leucite	K/K+Na = 0.82	H_2O	1.79	---	---
		P_2O_5	0.61	---	---
			98.68	99.4	100.0

1 Analyses made on an ETEC Autoprobe at the University of Massachusetts.

2 Analysis 1, p. 530, McBirney and Aoki (1968); FeO= FeO + .899Fe_2O_3.

3 Average of 10 probe analyses of fused basalt sample. Glass was prepared by fusing basalt in Mo foil under 10 bars pressure of H-N gas.

4 Mean of probe analyses of partially devitrified glassy patches probably representing late liquid; oxide analysis normalized to 100 percent. CIPW Norm: Ab 4.7, Or 44, Ne 39.5, Di 4.8, Ol 4.2, Ilm 1.4, Na_2SiO_3 1.6.

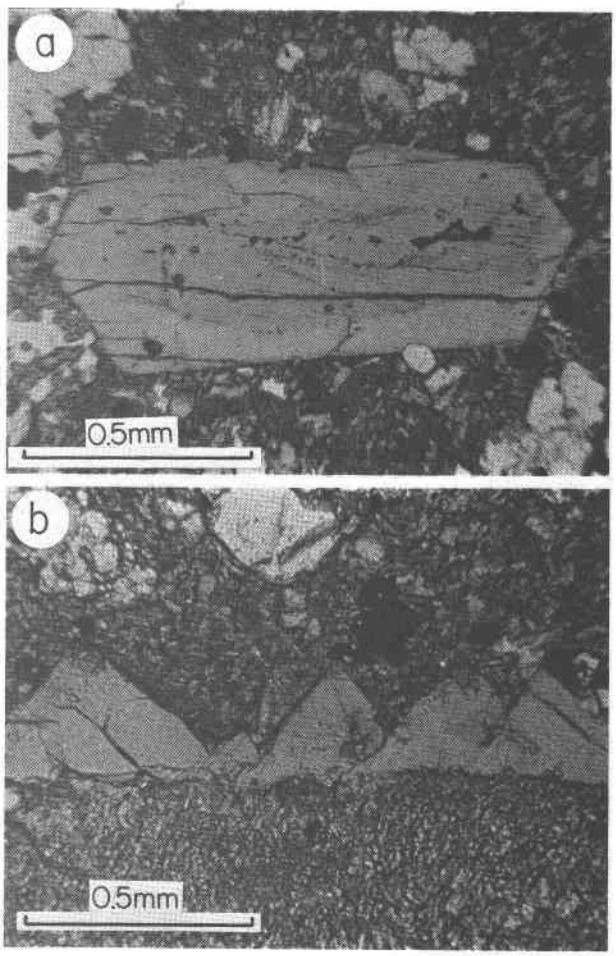

Fig. 1. (a) Zoned titanaugite phenocryst with relic skeletal interior (see text). (b) Zoned titanaugite overgrowth on lherzolite nodule.

may represent partially devitrified patches of late liquid (see analysis in Table 1).

While Ti has been thought to have the effect of lowering 2*V* (Dixon and Kennedy, 1933; Deer *et al.*, 1963), the lowest 2*V* observed in deeply-colored titanaugite was about 50°; the presence of other substitutions, especially acmite, may counteract the effect of Ti. The more deeply colored titanaugites have very strong inclined dispersion $r \gg v$.

Titanaugite chemistry

Electron microprobe analyses of titanaugites were done on two automated probes, a MAC-400 at Massachusetts Institute of Technology and an ETEC Autoprobe at the University of Massachusetts. Operating conditions included accelerating potential of 15 kV, beam current of 0.03 microamps, and spot size of about one micron. Standards used were synthetic jadeitic diopside glass JD-35 (Si, Ca, Mg, Na), spinel 52NL11 (Cr, Al), and ilmenite (Mn, Ti, Fe). Analyses were calculated from raw data using dead-time and drift corrections, and the correction procedure of Bence and Albee (1968) with the correction factors of Albee and Ray (1970).

Selected microprobe analyses of titanaugites are presented in Table 2. The analyses were chosen to illustrate the range of compositions found in titanaugite phenocrysts and overgrowths. Analysis 1 is typical of colorless cores and skeletal relics within larger phenocrysts, which are commonly richer in Cr than pyroxene which later crystallized around them. The phenocryst in Figure 1a contains such a skeletal relic, as shown by microprobe traverses. Analysis N is the average composition of augite within the spinel lherzolite nodules and lies outside the phenocryst zoning trends.

Below the analyses in Table 2 are listed the cations per 6 oxygens. In every case, the cation sum is greater than 4.0. In the formulas at the bottom of Table 2, the cations are normalized to 4.0 and additional oxygen is added to bring its sum to 6.0. For each amount of oxygen added, twice that amount of Fe^{2+} is converted to Fe^{3+} (see Finger, 1972). The resulting formulas have ferric iron contents ranging from 20 to 50 percent of total iron, which is in agreement with wet-chemical analyses of titanaugites from Tahiti published by McBirney and Aoki (1968). The above calculations assume that Fe is the only ion of variable valence and that the augite has ideal pyroxene stoichiometry. Titanium is considered to be Ti^{4+}. Although it is likely that Fe and Ti, once incorporated into the pyroxene structure, will exist in a state between $Fe^{2+}Ti^{4+}$ and $Fe^{3+}Ti^{3+}$ (Verhoogen, 1962; Burns, 1970), this does not affect the calculation of Fe and Ti in the structural formula. In fact, the values for Fe^{3+} in Table 2 should approximate the *minimum* contents of ferric iron, provided the basic assumptions are correct and the analyses are perfectly accurate.

In contrast to these analyses of terrestrial augites, those of lunar and Allende augites usually show cation sums per 6 oxygens of less than 4.0 (Mason, 1974; Papike *et al.*, 1974). Upon normalization to 4.0 cations, oxygen must be subtracted to bring the oxygen sum to 6.0. For each amount of oxygen thus subtracted, twice that amount of Ti^{4+} must be converted to Ti^{3+}. The presence of Ti^{3+} in lunar (Sung *et al.*, 1974) and Allende augites (Dowty and Clark, 1973) has been shown by spectrographic methods, and is consistent with the highly reducing conditions under

Table 2. Microprobe analyses of augite and titanaugite from Tahiti

	N*	1**	2	3	4	5	6	7	8	9	10
SiO_2	51.52	51.36	48.21	45.05	43.63	41.96	40.73	39.72	38.90	37.31	39.63
TiO_2	0.33	0.87	2.36	3.61	4.24	5.44	6.54	7.58	8.16	8.73	6.02
Al_2O_3	6.65	3.00	6.38	9.31	9.72	10.46	11.12	11.57	12.88	13.64	11.12
Cr_2O_3	0.82	0.87	0.84	0.30	0.03	0.02	0.03	0.07	0.10	0.06	0.28
FeO	3.67	6.60	5.95	7.01	7.71	8.06	9.79	10.46	9.42	9.40	12.57
MnO	0.14	0.18	0.09	0.16	0.16	0.20	0.30	0.23	0.28	0.22	0.26
MgO	15.88	15.15	13.79	12.09	11.35	10.13	8.37	7.88	8.30	7.58	6.60
CaO	19.50	21.33	22.74	22.54	22.36	22.00	21.45	21.70	22.10	21.56	20.60
Na_2O	1.36	0.54	0.44	0.51	0.63	0.64	1.24	1.08	1.19	1.13	1.11
	99.87	99.90	100.80	100.40	99.83	98.92	99.57	100.29	101.33	99.63	98.28
Cations per 6 oxygens											
Si	1.870	1.912	1.778	1.682	1.646	1.605	1.565	1.523	1.475	1.441	1.562
Al	.284	.131	.277	.401	.432	.473	.503	.521	.575	.620	.517
Ti	.009	.024	.065	.101	.120	.156	.189	.218	.233	.254	.178
Cr	.024	.025	.024	.009	.000	.000	.000	.002	.001	.001	.008
Mg	.859	.841	.758	.673	.638	.577	.479	.451	.469	.436	.388
Fe	.111	.205	.183	.218	.243	.257	.314	.335	.299	.304	.414
Mn	.004	.005	.002	.004	.005	.006	.009	.007	.009	.007	.008
Ca	.758	.851	.899	.901	.904	.901	.883	.892	.898	.892	.871
Na	.096	.038	.031	.036	.046	.047	.092	.080	.088	.075	.085
	4.015	4.032	4.017	4.025	4.034	4.022	4.034	4.029	4.047	4.030	4.031
Formulas per 4 cations											
Si	1.863	1.897	1.770	1.672	1.632	1.596	1.552	1.512	1.457	1.430	1.549
Al	.137	.103	.230	.328	.368	.404	.448	.488	.543	.570	.451
	2.000	2.000	2.000	2.000	2.000	2.000	2.000	2.000	2.000	2.000	2.000
Al	.146	.027	.046	.071	.060	.066	.051	.029	.025	.045	.061
Ti	.009	.024	.065	.100	.119	.155	.187	.216	.230	.252	.177
Cr	.024	.025	.024	.009	.000	.000	.000	.002	.001	.001	.008
Fe^{3+}	.044	.040	.060	.082	.116	.074	.114	.102	.144	.098	.114
Mg	.777	.834	.755	.669	.633	.574	.475	.450	.464	.433	.385
Fe^{2+}	.000	.050	.050	.069	.072	.131	.173	.201	.136	.171	.255
	1.000	1.000	1.000	1.000	1.000	1.000	1.000	1.000	1.000	1.000	1.000
Mg	.079										
Fe^{2+}	.067	.113	.072	.066	.053	.051	.024	.028	.016	.033	.044
Mn	.004	.005	.002	.004	.005	.006	.009	.007	.009	.007	.008
Ca	.755	.844	.895	.894	.896	.896	.876	.886	.888	.886	.864
Na	.095	.038	.031	.036	.046	.047	.091	.079	.087	.074	.084
	1.000	1.000	1.000	1.000	1.000	1.000	1.000	1.000	1.000	1.000	1.000

* *Typical augite in spinel lherzolite nodule.*

** *Colorless core of titanaugite phenocryst.*

which these pyroxenes formed. It must be emphasized, however, that these normalization schemes should be viewed with some caution, since they are being applied to rapidly crystallized pyroxenes which may violate the assumption of ideal stoichiometry.

Examination of the analyses in Table 2 reveals that the compositional changes are systematic. Aluminum and total iron increase with increasing titanium, while magnesium and silicon decrease and calcium remains constant. The earliest, most magnesian augite contains some Cr, but the crystallizing magma was apparently rapidly depleted in Cr. Enrichment of Na in later-crystallized augite, probably as acmite and minor $NaTiAlSiO_6$, reflects the alkali enrichment of the residual liquid. Such systematic behavior does not necessarily indicate the stability of high-Ti pyroxene substitutions, but does suggest that they are crystal-chemically controlled, even though their incorporation into growing pyroxene crystals may be through metastable addition of a surface adsorption layer (Dowty, 1976). Analyses of several small sector-zoned crystals show that element profiles from center to edge in the (100) and ($\bar{1}11$) sectors are similar in shape, though (100) is richer in Ti, Al, and Fe, and poorer in Mg and Si. Substitution *trends,* however, are the same in both sectors, as also noted by Downes (1974).

Pyroxene subsitutions

The simplest structural formula for calcic clinopyroxene may be taken as that of diopside, $CaMgSi_2O_6$, where Ca is in the large ($M2$) site, Mg is in the ($M1$) octahedral site, and Si is tetrahedrally coordinated. Simple substitutions of Fe^{2+}, Mg, and Mn for Ca in ($M2$) and Fe^{2+} and Mn^{2+} for Mg in ($M1$) give rise to the compositional variations described in the familiar "pyroxene quadrilateral," plotted as proportions of $CaSiO_3$, $MgSiO_3$, and $(Fe,Mn)SiO_3$ and usually calculated from atomic proportions of Ca, Mg, and (Fe + Mn). When the Tahitian augite analyses are calculated in this manner, some of them seem to show greater than 50 percent $CaSiO_3$ (Wo). This is because of the exclusive subsitution of "non-quadrilateral" components such as Ti, Al, Cr, and Fe^{3+} for Fe^{2+} and Mg in ($M1$) as discussed below.

More complex substitutions involve replacement of Ca, Mg, and Si by ions of different valence in each of the three sites in a combination that preserves charge balance:

$$Ca_{1-x}R_x^{1+}Mg_{1-y}R_y^{3+}Si_{2-z}R_z^{3+}O_6, \text{ where } x + z = y.$$

The x charge-reducing substitution in ($M2$) usually involves Na for Ca. The Tahitian augites (Table 2) have Na ranging from 0.031 to 0.098.[3] The z charge-reducing substitution in tetrahedral sites involves Al^{3+}, less commonly Fe^{3+}, for Si. There is reasonable evidence from structural studies that Ti^{4+} does not enter substantially into tetrahedral sites of pyroxenes where Al or Fe^{3+} is available (*e.g.* Dowty and Clark, 1973). In the Tahitian pyroxenes (Table 2), the z substitution is assumed to be entirely Al and ranges from 0.102 to 0.599. In Figure 2 (top), relations between the x and z charge-reducing substitutions are shown for the Tahitian augites. A very wide range of tetrahedral Al is accompanied by nearly constant Na, except for a step-like increase in many of the most silica-deficient compositions.

The y charge-increasing substitutions in ($M1$) involve trivalent ions such as Al^{3+}, Cr^{3+}, Fe^{3+}, and Ti^{3+} for Mg. In addition, quadrivalent ions, in particular Ti^{4+}, may substitute in the ($M1$) site. Each amount of such Ti^{4+} substitution contributes twice as much charge increase as an equivalent amount of a trivalent ion, hence the amount of Ti^{4+} must be doubled in computing y. Alternatively, Ti^{4+} may be considered to be combined with Mg or Fe^{2+} to give two "mean trivalent ions" in much the same way that ilmenite is related to corundum. The relation of y charge-increasing and z charge-reducing substitutions is illustrated in the lower part of Figure 2, for Tahitian augites.

Figures 3 and 4 illustrate the nature of y substitutions in titanaugites. In Figure 3, the total calculated occupancy of the ($M1$) site is expressed in terms of R^{2+} and two types of y substitutions: R^{3+} (which includes Al, Cr, and Fe^{3+}) and $2Ti^{4+}$. Since each Ti^{4+} requires an R^{2+} ion to make two "mean trivalent" ions, Ti^{4+} is subtracted from the amount of R^{2+}.[4] It is evident from Figure 3, as well as from the bottom of Table 2, that the Tahiti augites vary only slightly in the R^{3+} substitution from a low of 0.092 for the least titaniferous augites to values close to the average of 0.161 for the rest of the trend. Thus the principal y variation is in the $2Ti^{4+}$ substitution from a low of 0.048 to a maximum of 0.506 (25.3 percent of $M1$ sites occupied by Ti^{4+}). This is further emphasized in the right-hand side of Figure 4, in which proportions of three y substitutions, Al + Cr, Fe^{3+}, and $2Ti^{4+}$ are portrayed. The location of points in this figure is heavily dependent on minor analytical variations, particularly in SiO_2 and Al_2O_3, which influence calculated amounts of octahedral Al and Fe^{3+}. As the total y substitution increases (shown by increasing size of symbols in Fig. 4), the percentage of $2Ti^{4+}$ increases to a maximum of 78 percent.

In recent studies of zoned titanaugites (Bence and Papike, 1972; Papike *et al.*, 1974; Downes, 1974), diagrams have been presented showing Ti *vs.* Al, and slopes of linear trends on such diagrams have been

---

[3] These and following values are based on 4 cation–6 oxygen formulas and are taken from selected analyses used for plotting purposes, of which those in Table 2 are a representative selection.

[4] Note that on this basis, the ideal end member $CaTiAl_2O_6$ plots at +2.00 ($2Ti^{4+}$) and −1.00 ($R^{2+} - Ti^{4+}$).

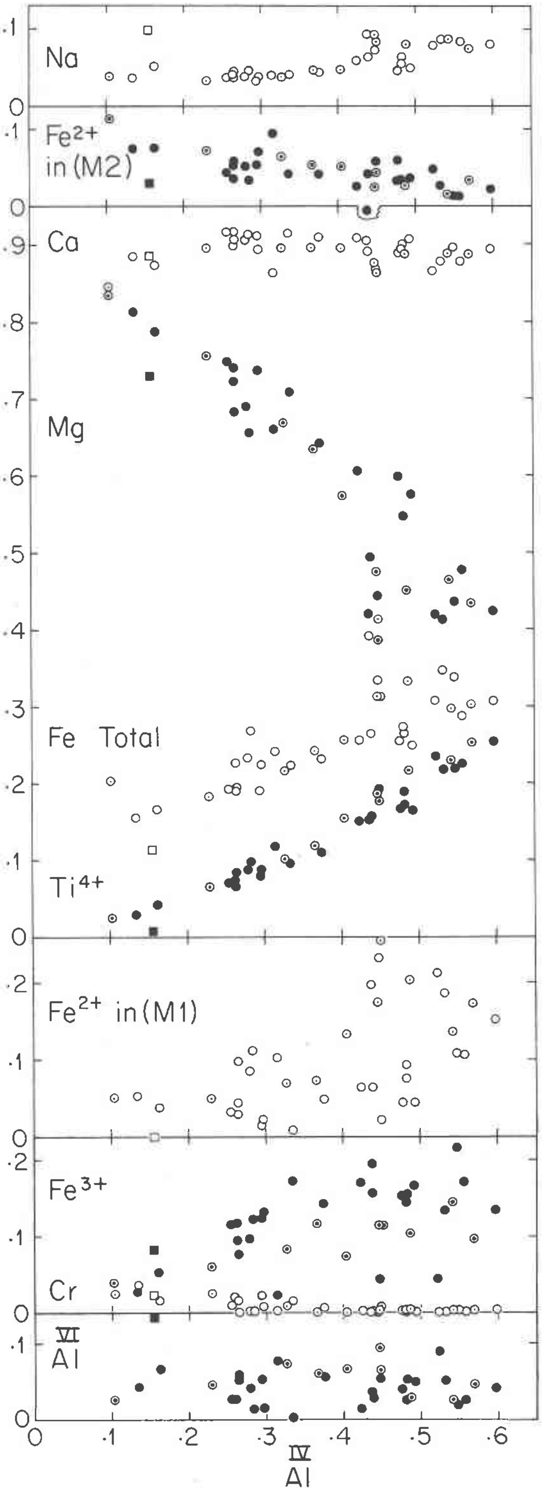

Fig. 2. Relations between various cations and tetrahedral Al in Tahitian augites, based on a stoichiometric formula of four cations and six oxygens. The top part of the figure shows the cations important in ($M2$), while the lower part illustrates the substitutions in ($M1$). Analyses from Table 2 are shown as open circles with dots.

used to suggest titanium substitution mechanisms. Such a plot for the Tahitian augites (Fig. 5) shows a linear trend with a slope of 1/2, suggesting substitution toward an $R^{2+}TiAl_2O_6$ composition. This, and the small change of Na with increasing Ti (see Fig. 2 and Table 2) indicates relatively little involvement of the $NaTiAlSiO_6$ substitution suggested by Hollister and Gancarz (1971). In Figure 5 the zero Ti intercept lies at Al = 0.13, quite close to the mean amount of Al calculated to be involved in other substitutions. This includes y substitution of Al in ($M1$) (mean = 0.043) plus the mean amount of z substitution of Al for Si (mean = 0.104) that is required to compensate for the y substitutions of Al, Fe^{3+}, and Cr^{3+} (mean = 0.161) that are not already compensated by x substitution of Na (mean = 0.057).

Diagrams such as Figure 5 might be used to support a coupled substitution: Ti^4 + 2Al for (Mg,Fe^{2+})+2Si, leading to an idealized pyroxene end-member $CaTiAl_2O_6$. Such a substitution implies, other things being equal, that the sum of Ti^{4+} and (Mg + Fe) in ($M1$) should remain constant at 1.0 minus any other cations present in ($M1$), and that the data should form a line of −1.0 slope in a plot of Ti *vs.* (Mg + Fe). Figure 6, however, shows a slope of −0.7 for the Tahitian augites. Strictly speaking, the Fe in Figure 6 should be Fe^{2+} in ($M1$), but since we cannot calculate this without some uncertainty and since calculated Fe^{2+} and Fe^{3+} in ($M2$) do not vary with increasing Ti content (Fig. 2), total Fe has been used in the plots of Figure 6. While the plot in Figure 6 (top) does not indicate a simple relationship, the plot in Figure 6 (bottom) of (Ti+Fe) *vs.* Mg yields a line of −1.0 slope. This supports a proposed substitution: $Fe^{2+}+Ti^{4+}+2Al$ for 2Mg+2Si, leading to an idealized end-member $CaFe^{2+}_{0.5}Ti^{4+}_{0.5}AlSiO_6$. It should be emphasized that the linear trend shown in Figure 6 (bottom) is not *proof* that the relationship is controlled by crystal chemistry. It is reasonable, for example, that the relationship between Fe^{2+} and Ti^{4+} enrichment in the melt, partially controlled by crystallization of other phases such as olivine and oxides, was just right to produce the relation observed in the augite. If, on the other hand, the relation is a function of augite crystal chemistry, then it could have serious effects on magmatic crystallization trends. There is also the possibility that Fe^{2+} could be of key importance in enhancing the solubility of Ti^{4+} in pyroxene, as well as in other silicates. An interesting feature of the hypothetical $Fe^{2+}Ti^{4+}$ end-member (and of its MgTi analog) is the possibility of coupled ordering of Fe^{2+} and Ti^{4+} in alternate ($M1$) positions.

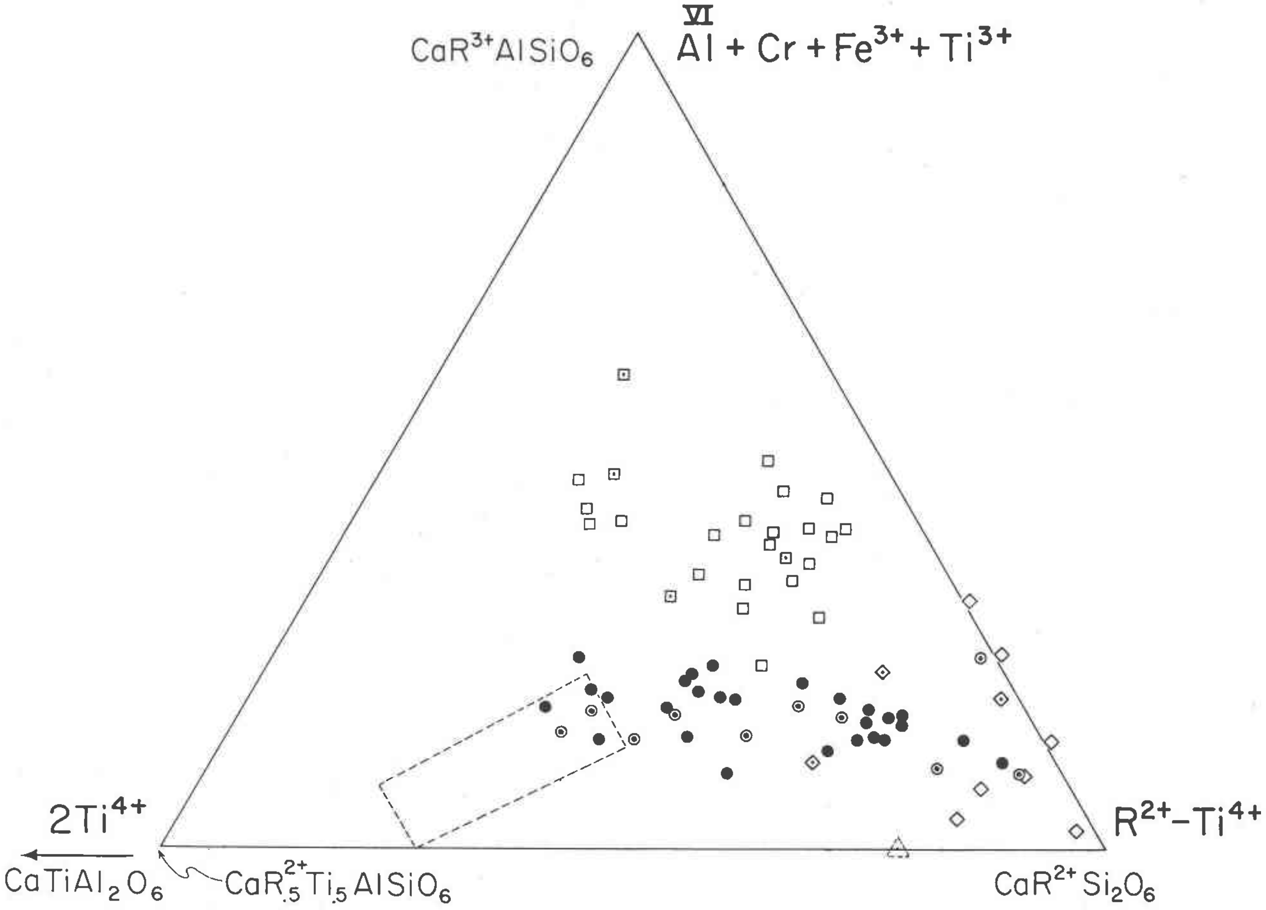

Fig. 3. Plot showing total calculated occupancy of the (*M*1) site in titanaugites from Tahiti (circles), Allende meteorite (squares), and lunar basalts (diamonds). Analyses from Tables 2 and 3 are shown with internal dots. Allende data from Mason (1974) and Grossman (1975); lunar data from Papike *et al.* (1974), Agrell *et al.* (1970), Bunch *et al.* (1970) and Frondel (1975). Large dashed rectangle represents compositional range of Yang (1973); small triangle is the limit of compositions reported by Yagi and Onuma (1967). Note that the Tahiti trend includes the most Ti^{4+}-rich augites yet reported, and the Allende meteorite has the most Ti^{3+}-rich.

Other examples of Ti-rich augite

As pointed out in the introduction, other augites with Ti content comparable to or higher than those from Tahiti are reported from the Moon, from Allende meteorite, and from some experimental syntheses. Some typical examples are listed in Table 3. In most cases, normalization of probe analyses to 4 cations results in a substantial amount of calculated Ti^{3+}, and several spectrographic studies, including that of Dowty and Clark (1973) on specimen F, strongly indicate the presence of Ti^{3+} as well as Ti^{4+}. As can be seen in Figure 3, lunar and Allende augites are grouped in a broad trend from $R^{2+}-Ti^{4+}$ toward R^{3+}, with a maximum of 58 percent R^{3+} and a maximum of 35 percent $2Ti^{4+}$. In contrast, the Tahitian augites do not quite attain 25 percent R^{3+} but extend to nearly 51 percent $2Ti^{4+}$.

Subdivision of the *y* substitutions in lunar and Allende augites is shown in the left half of Figure 4. As might be expected, considering the analytical uncertainties, there is considerable scatter, but with fairly tight clustering of the most extremely substituted Allende augites. The nature of substitution in Allende augites is well shown in Figure 7, which shows a plot of various ions in the formula *vs.* tetrahedral Al, as was done for Tahitian augites in Figure 2. Most striking is the positive correlation of Ti^{3+} with tetrahedral Al, with a ratio of 1.1/1. Ti^{4+} correlates with tetrahedral Al with a small ratio of 0.2/1. These compare to negative correlations between Mg and tetrahedral Al of 0.8/1 and between octahedral and tetrahedral Al of 0.5/1. This suggests that for every five ions of Ti^{3+} introduced, two substitute directly for octahedral Al, while three substitute for Mg, requiring additional coupled substitution of Al

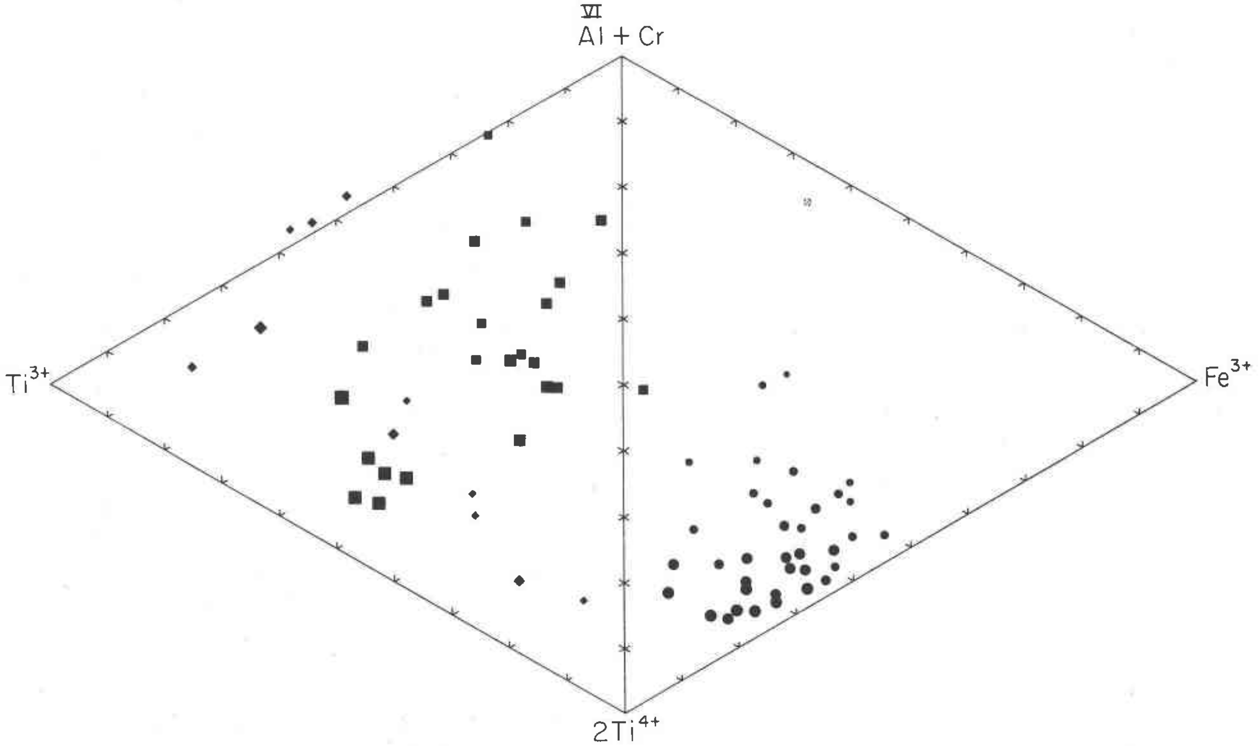

Fig. 4. Proportions of cations involved in *y* substitutions in (*M*1), calculated from stoichiometry. Circles—Tahiti; squares—Allende; diamonds—lunar basalts. Data sources are the same as in Figure 3. Size of symbols is proportional to the extent of *y* substitution, the largest symbols indicating the largest substitution.

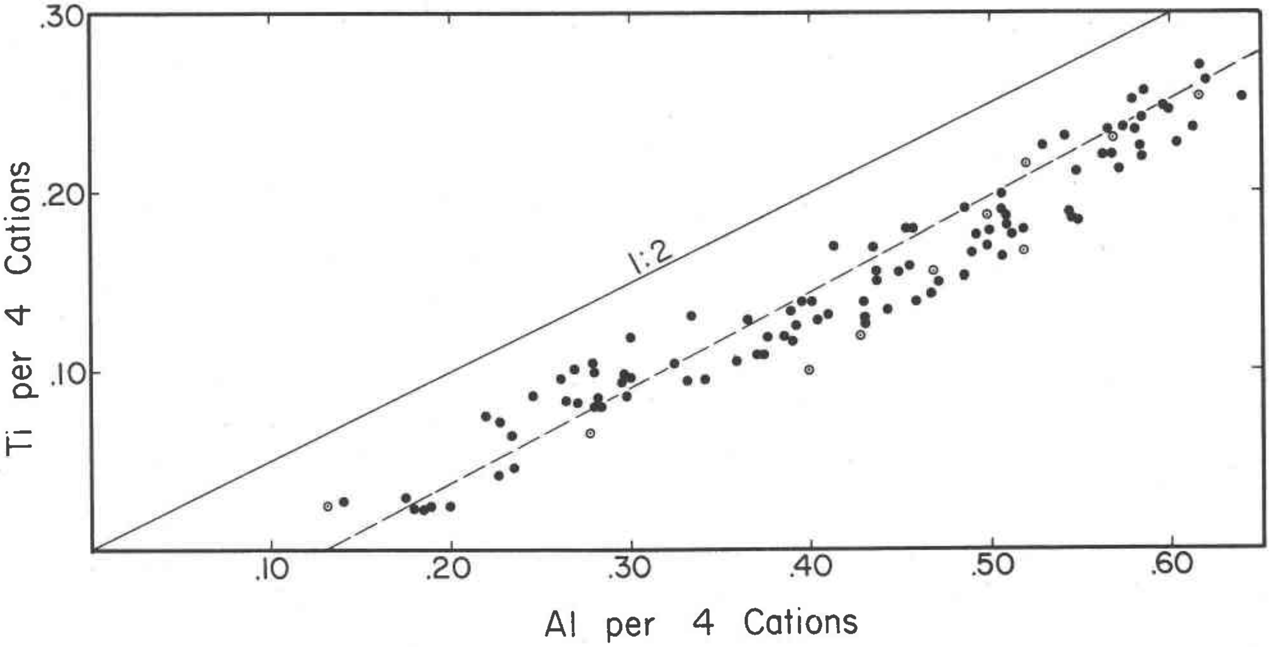

Fig. 5. Plot of Ti *vs.* Al for Tahitian augites. Open symbols with dots are analyses from Table 2. The ideal 1:2 line is shown, along with the calculated least-squares best fit for the data (dashed line), which has the equation Al = 1.86 Ti + 0.13.

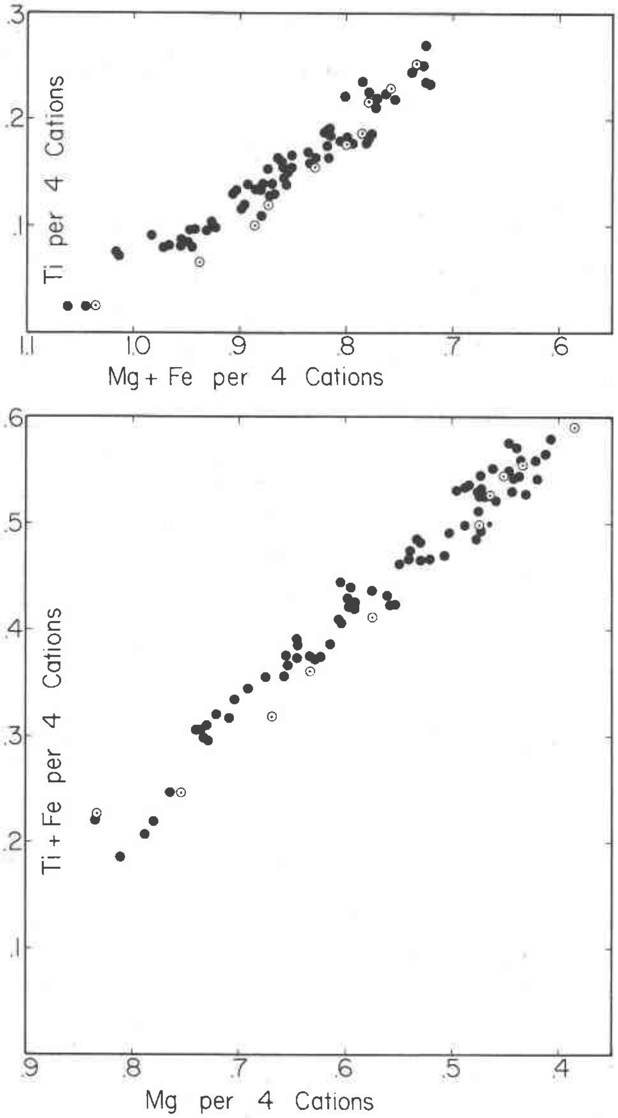

Fig. 6. Plots showing negative correlation between Ti and (Mg+Fe) and between (Ti+Fe) and Mg. Open symbols with dots are analyses from Table 2. The slope of the data in the upper plot is approximately −0.7 (note reversed abscissa scale), and that in the lower plot is almost exactly −1.0. In both cases, Fe is total Fe (see text).

for Si. The two generalized compositions on the two ends of the Allende series shown are then:

$$Ca_{1.00}(Mg_{0.63}Al_{0.30}Ti^{4+}_{0.07})(Al_{0.44}Si_{1.56})O_6$$

$$Ca_{1.00}(Mg_{0.36}Al_{0.11}Ti^{4+}_{0.15}Ti^{3+}_{0.38})(Al_{0.80}Si_{1.20})O_6.$$

The limited number of lunar augites from diverse sources studied by us does not show such clear patterns.

Yagi and Onuma (1967) performed experiments on the join $CaMgSi_2O_6$–$CaTiAl_2O_6$ at 1 atmosphere and found a maximum solubility of $CaTiAl_2O_6$ in diopside (coexisting with perovskite and corundum) equivalent to 3.7 weight percent TiO_2. On the other hand, Yang (1973) reports experiments in the system $CaMgSi_2O_6$–$CaTiAl_2O_6$–$CaAlAlSiO_6$ in which he produced augites on the liquidus at 1235–1245°C which contained 8–16 weight percent TiO_2 and 16–20 weight percent Al_2O_3. Assuming all Ti was Ti^{4+} in these experimental products (for which synthesis fO_2 conditions were not reported), as Yang contends, the compositional limits greatly exceed all natural pyroxenes except those of the Allende meteorite. Yang's compositions, however, may be metastable, as indicated by the rod-like exsolutions of perovskite and corundum which he reports in some of his synthetic pyroxene crystals. If the composition of Yagi and Onuma (1967) is taken to be more nearly that of

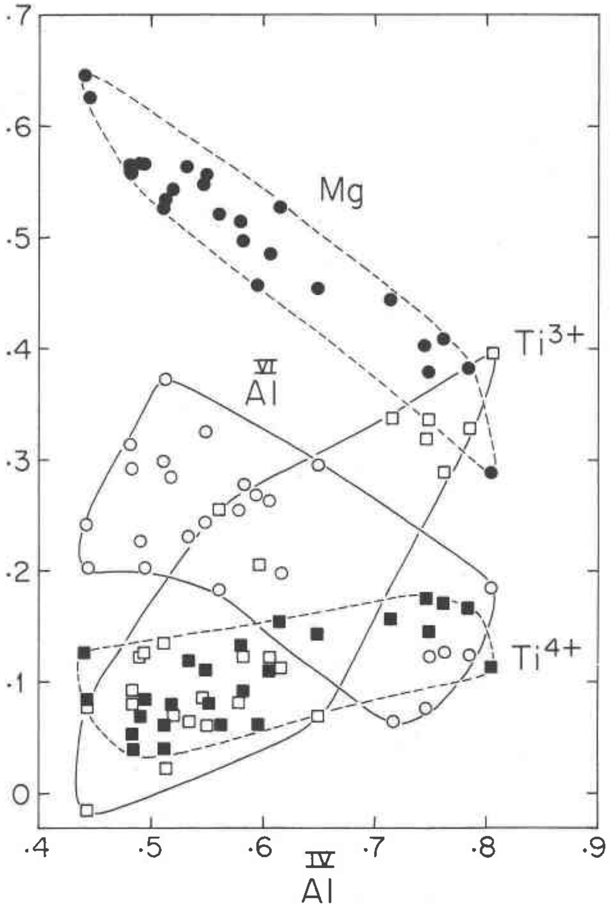

Fig. 7. Substitution trends in Allende augites based on ideal pyroxene stoichiometry. Mg—filled circles; Al—open circles; Ti^{3+}—open squares; Ti^{4+}—closed squares. Data from Mason (1974) and Haggerty (personal communication, 1976).

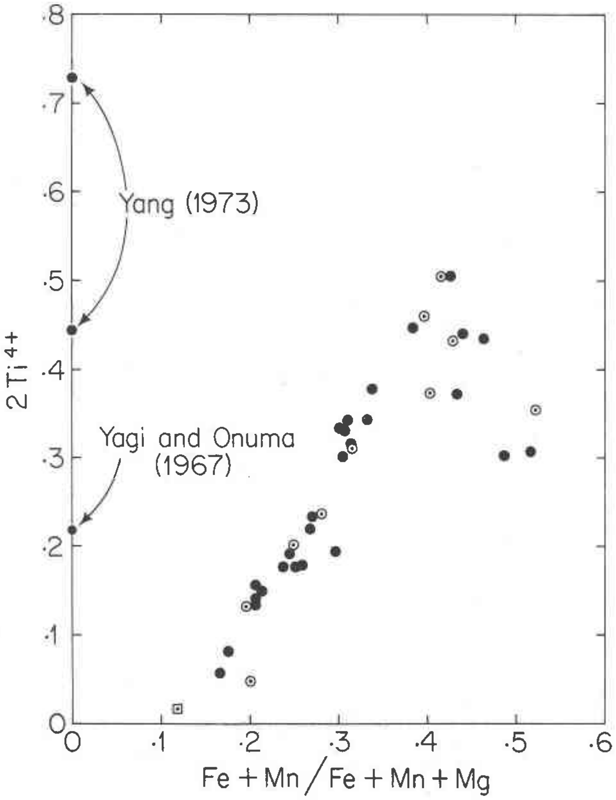

Fig. 8. Relation between 2 Ti^{4+} and the ratio (Fe+Mn)/(Fe+Mn+Mg) (used as a differentiation index) in Tahitian augites. Square indicates augite from lherzolite nodule (analysis N, Table 2); dotted symbols indicate analyses in Table 2.

stable-equilibrium iron-free clinopyroxene, this implies that Fe^{2+}–Ti^{4+} coupling might be required to produce more Ti-rich *stable* pyroxene compositions. The results of Yang (1973) imply that Fe^{2+}–Ti^{4+} coupling is not necessarily important in producing *metastable* Ti-rich compositions. All the above observations, of course, are dependent on the fO_2 dependence of titanium substitutions, which has not been adequately characterized experimentally.

Conditions for crystallization of Ti-rich augite

The apparent rarity in terrestrial basalts of titanaugites as rich in titanium as those reported here may simply reflect the difficulty of recognizing these unusual compositions without exhaustive microprobe analysis. This study has provided an opportunity to determine the physical and chemical conditions which promote the crystallization of such titaniferous augites.

Examination of reported occurrences shows that low silica activity is an important factor in formation of titanaugite: most titanaugite occurrences are in alkali olivine basalts and other alkali-rich, silica-poor igneous rocks. In addition, a liquid composition rather high in titanium is required, though residual interstitial liquids sufficiently rich in titanium could be produced from magmas with only modest Ti contents. A bulk chemical analysis of the Tahitian basalt (Table 1) indicates the low SiO_2 and rather high TiO_2. Al_2O_3 is low with respect to CaO, so that early precipitates from the melt were olivine, low-Ti augite, and Mg–Cr–Al spinel, and plagioclase appeared relatively late. Early crystallization of these magnesian phases caused a progressive increase in Fe/Mg ratio and Ti content of the residual liquid, resulting in precipitation of increasingly titaniferous spinel and ultimately ilmenite, which eventually stopped further Ti enrichment in melt and in titanaugite. This specimen is unusual in the very high initial Mg/Fe ratio combined with low oxygen fugacity, which delayed precipitation of titaniferous magnetite and ilmenite until the melt had reached extremely high Ti content. Ultimately, however, these phases did crystallize, and the outermost rims on some augites with the highest Fe/Mg ratios (*e.g.* analysis 10, Table 2) show Ti content less than the maximum. This is illustrated in Figure 8, in which titanium substitution is plotted against the ratio (Fe+Mn)/(Fe+Mn+Mg)(=*fe*), which serves as a differentiation index. The Ti enrichment trend begins at *fe* = 0.15 and proceeds to maximum titanium (0.252) at *fe* = 0.42. Beyond this, Ti drops to about 0.175 while *fe* increases to 0.52.

The titanaugites of Tahiti, similar to many other reported titanaugites, occur in an environment where metastable crystallization could be suspected. The stability of high-Ti augites has been questioned by Hollister and Gancarz (1971) and Dowty (1976) because of the common occurrence of sector-zoning. These authors have suggested that crystallization rate is just as important a variable as magma chemistry in the formation of titaniferous augites. The Tahitian titanaugites are enigmatic in that sector-zoning is rather rare. Though sector-zoned augites do occur, and though the *most* Ti-rich compositions occur in the (100) sectors of these crystals, there are abundant augite phenocrysts without sector-zoning that contain over 7 weight percent TiO_2. Rapid cooling and rapid crystallization, in addition to promoting possible metastable crystal growth, may also produce the extreme residual liquid compositions which appear to be required to crystallize Ti-rich augites.

In summary, the above observations suggest that these Ti-rich augites are the product both of special

Table 3. Microprobe analyses of lunar and Allende meteorite titanaugites

	LUNAR*			ALLENDE**		
	1	2	3	D	F	I
SiO_2	42.3	43.1	42.74	37.2	32.8	31.3
TiO_2	9.3	7.13	6.57	9.2	16.6	17.7
Al_2O_3	9.1	9.04	8.77	18.3	19.3	22.0
Cr_2O_3	0.34	0.44	0.64			
FeO	16.4	11.0	9.28	0.0	<0.1	0.0
MnO	0.38		0.19			
MgO	7.5	10.1	10.71	9.4	6.7	5.1
CaO	13.5	19.1	20.58	24.6	24.6	24.9
Na_2O	0.43		0.12			
K_2O	0.20					
	99.45	99.9	99.60	98.7	100.0	101.0
Formulas based on 4 cations						
Si	1.674	1.654	1.633	1.384	1.251	1.196
Al	.326	.346	.367	.616	.749	.804
	2.000	2.000	2.000	2.000	2.000	2.000
Al	.098	.064	.028	.198	.123	.186
Ti^{4+}	.020	.065	.129	.153	.146	.111
Ti^{3+}	.257	.141	.060	.112	.336	.394
Cr	.012	.013	.019			
Mg	.443	.577	.610	.529	.379	.289
Fe^{2+}	.170	.140	.154	.000	.000	.000
Mn	.000		.000			
Ca				.008	.015	.021
	1.000	1.000	1.000	1.000	1.000	1.000
Fe^{2+}	.373	.212	.143			
Mn	.012		.006			
Ca	.573	.787	.843	1.000	1.000	1.000
Na	.033		.009			
K			.010			
	1.001	.999	1.001	1.000	1.000	1.000

* *(1) Apollo 11, Bunch et al. (1970); (2) Apollo 17, Papike et al. (1974), p. 483, anal. 5; (3) Apollo 17, Frondel (1975) p. 236, anal. 5.*

***All reported in Mason (1974).*

magma chemistry and rapid crystallization. It is ambiguous whether the titanaugite compositions are metastable due to rapid crystallization or are products of residual liquids which resulted from it. We cannot comment on the stability of the Ti-rich augite compositions reported here, but can only point to the systematic behavior of the compositional trends. These may be functions of a crystal-chemical control or may reflect changing liquid composition.

Acknowledgements

We thank David Walker, Edward Stolper, Lincoln Hollister, and Eric Dowty for reviews and helpful comments on this manuscript. We also thank the National Science Foundation for support for one of us (RJT) through grant DES-75-15012 and for support of the microprobe facility at the University of Massachusetts.

References

Agrell, S. O., J. H. Scoon, I. D. Muir, J. V. P. Long, J. D. C. McConnell and A. Peckett (1970) Observations on the chemistry, mineralogy and petrology of some Apollo 11 lunar samples. *Proc. Apollo 11 Lunar Science Conf.*, 93–128.

Albee, A.L. and L. Ray (1970) Correction factors for electron probe microanalysis of silicates, oxides, carbonates, phosphates and sulfates. *Anal. Chem.*, *42*, 1408–1414.

Bence, A. E. and A. L. Albee (1968) Empirical correction factors for the electron microanalysis of silicates and oxides. *J. Geol.*, *76*, 382–403.

——— and J. J. Papike (1972) Pyroxenes as recorders of lunar basalt petrogenesis: chemical trends due to crystal-liquid interaction. *Proc. Third Lunar Sci. Conf.*, 431–468.

Brown, G. M., A. Peckett, R. Phillips and C. H. Emeleus (1975) Mineralogy and petrology of Apollo 17 basalts [Abstr.]. *Sixth Lunar Sci. Conf.*, p. 95.

Buddington, A. F. and D. H. Lindlsey (1964) Iron-titanium oxide minerals and synthetic equivalents. *J. Petrol.*, *5*, 310–357.

Bunch, T. E., K. Keil and M. Prinz (1970) Electron microprobe analysis of pyroxenes, plagioclases, and ilmenites from Apollo 11 lunar samples. *Univ. New Mexico Spec. Pub. 1*, 1–19.

Burns, R. G. (1970) *Mineralogical Applications of Crystal Field Theory*, Cambridge University Press, Cambridge, England.

Deer, W. A., R. A. Howie and J. Zussman (1963) *Rock-Forming Minerals*, Vol. 2: *Chain Silicates*. Longmans, Green and Company Ltd., London.

Dixon, B. E. and W. Q. Kennedy (1933) Optically uniaxial titanaugite from Aberdeenshire. *Z. Kristallogr.*, *86*, 112–120.

Downes, M. J. (1974) Sector and oscillatory zoning in calcic augites from Mt. Etna, Sicily. *Contrib. Mineral. Petrol.*, *47*, 187–196.

Dowty, E. (1976) Crystal structure and crystal growth: II. Sector zoning in minerals. *Am. Mineral.*, *61*, 460–469.

——— and J. R. Clark (1973) Crystal structure refinement and optical properties of a Ti^{3+} fassaite from the Allende meteorite. *Am. Mineral.*, *58*, 230–242.

Dymond, J. (1975) K–Ar ages of Tahiti and Moorea, Society Islands, and implications for the hot-spot model. *Geology*, *3*, 236–240.

Finger, L. W. (1972) The uncertainty in the calculated ferric iron content of a microprobe analysis. *Carnegie Inst. Wash. Year Book*, *71*, 600–603.

Frondel, J. W. (1975) *Lunar Mineralogy*. John Wiley and Sons, Inc. New York.

Fuchs, L. (1971) Occurrence of wollastonite, rhönite, and andradite in the Allende meteorite. *Am. Mineral.*, *56*, 2053–2068.

Grossman, L. (1975) Petrography and mineral chemistry of Ca-rich inclusions in the Allende meteorite. *Geochim. Cosmochim. Acta*, *39*, 433–454

Hollister, L. S. and A. J. Gancarz (1971) Compositional sector-zoning in clinopyroxene from the Narce area, Italy. *Am. Mineral.*, *56*, 959–979.

Lebedev, P. I. and A. P. Lebedev (1934) The titanite–magnetite gabbro mass Patyn (Western Siberia). *Doklady Acad. Sci. USSR*, *3*, 294–296.

McBirney, A. R. and K. Aoki (1968) Petrology of the island of Tahiti. In R. R. Coats, R. L. Hay and C. A. Anderson, Eds.

Studies in Volcanology: A Memoir in Honor of Howell Williams, Geol. Soc. Am. Mem., 116, 523–556.

Mason, B. (1974) Aluminum–titanium-rich pyroxenes, with special reference to the Allende meteorite. *Am. Mineral., 59,* 1198–1202.

Papike, J. J., A. E. Bence and D. H. Lindsley (1974) Mare basalts from the Taurus-Littrow region of the moon. *Proc. Fifth Lunar Science Conf.,* 471–504.

Strong, D. F. (1969) Formation of the hour-glass structure in augite. *Mineral. Mag., 37,* 472–479.

Sung, C.-M., R. M. Abu-Eid and R. G. Burns (1974) Ti^{3+}/Ti^{4+} ratios in lunar pyroxenes: Implications to depth of origin of mare basalt magma. *Proc. Fifth Lunar Sci. Conf.,* 717–726.

Tracy, R. J. and Peter Robinson (1975) Spinel lherzolite nodules from Tahiti: reaction rims and titanaugite overgrowths against enclosing alkali olivine basalt. *Trans. Am. Geophys. Union, 56,* 464.

Verhoogen, J. (1962) Distribution of titanium between silicates and oxides in igneous rocks. *Am. J. Sci., 260,* 211–220.

Williams, H. (1933) Geology of Tahiti, Moorea and Maiao. *Bishop Mus. Bull., 105,* 89 p.

Yagi, K. and K. Onuma (1967) The join $CaMgSi_2O_6$–$CaTiAl_2O_6$ and its bearing on the titanaugites. *J. Fac. Sci. Hokkaido Univ., Ser. IV, 13,* 463–483.

Yang, H.-Y. (1973) Synthesis of an Al- and Ti-rich clinopyroxene in the system $CaMgSi_2O_6$–$CaAl_2SiO_6$–$CaTiAl_2O_6$. *Trans. Am. Geophys. Union, 54,* 478.

Manuscript received, August 25, 1976; accepted for publication, February 3, 1977.